A new approach to formulation of complex fuel surrogates

Al-Esawi, N. H. I. & Al Qubeissi, M.

Original citation & hyperlink:
Al-Esawi, NHI & Al Qubeissi, M 2021, 'A new approach to formulation of complex fuel surrogates', Fuel, vol. 283, 118923.
https://dx.doi.org/10.1016/j.fuel.2020.118923

DOI 10.1016/j.fuel.2020.118923
ISSN 0016-2361

Publisher: Elsevier

A new approach to formulation of complex fuel surrogates

Nawar Al-Esawi[1,2*], Mansour Al Qubeissi[2,3]

[1]*Faculty of Arts, Science and Technology, University of Northampton, Northampton, NN1 5PH, UK*
[2]*Institute for Future Transport and Cities, Coventry University, Coventry. CV1 5FB, UK*
[3]*Faculty of Engineering, Environment and Computing, Coventry University, Coventry, CV1 2JH, UK*
[*] Corresponding author: Nawar.Al-Esawi@northampton.ac.uk

Abstract

This paper presents a new approach to the formulation of fuel surrogates in application to gasoline, diesel, and their biofuel blends (including blends of biodiesel/diesel and ethanol/gasoline). This new approach, described as a 'Complex Fuel Surrogates Model (CFSM)', is based on a modified version of the Multi-Dimensional Quasi-Discrete Model (MDQDM). The new approach is aimed to reduce the full composition of fuel to a much smaller number of components based on their mass fractions to formulate fuel surrogates. The formulated surrogates for gasoline and blended ethanol/gasoline fuels matched the data of the full compositions of the same fuels for droplet lifetime, surface temperature, density, vapour pressure, H/C ratio, molar weight and research octane number, using the CFSM. Also, the cetane number and viscosity of diesel and biodiesel/diesel blends were mimicked by their suggested surrogates. The results were verified, with up to 7.2% errors between the two sets of predicted droplet lifetimes: surrogates and full compositions of fuels.

Keywords: Biodiesel; Combustion; Diesel; Ethanol; Fuel surrogates; Gasoline

1. Introduction

Commercial fuels are complex mixtures of many hydrocarbon components [1,2]. Due to the lack of chemical data and the complexities of the combustion processes of these fuels (including heating, evaporation and ignition), and the consequences of computationally-expensive models, surrogates (a much smaller number of components) are introduced to match the physical and chemical behaviours of the original fuel composition. A wide range of fuel surrogates have been formulated to emulate either the physical or chemical behaviours of the full fuel compositions [3–12].

Due to the lack of chemical data and the limitations of the computational resources, in some studies (e.g., [13–16]), fuels were approximated with single components; e.g., diesel and gasoline fuels were

represented by n-dodecane and iso-octane, respectively. However, as the chemical mechanisms and the computational efficiency became compatible for a wider range of components, researchers started to approximate fuels by a reasonably higher number of components to mimic the desirable characteristics of fuel.

Mati et al. [3] approximated diesel fuel by 5 components and the yielded kinetics of oxidation were in a good agreement with those for diesel fuel. Sarathy et al. [5] suggested two surrogates for gasoline FACE A (Fuel used in Advanced Combustion Engines, Type A) and FACE C. Surrogates of five and six components were suggested for FACE A and FACE C gasoline fuels, respectively. A very good agreement was obtained in [5] between the suggested surrogates and the real fuels for the predictions of their ignition time delays, Research Octane Numbers (RONs), Motor Octane Numbers (MONs), Hydrogen to Carbon ratios (H/C) and average Molar Weights (MWs) . The latter work was further advanced in [6] by suggesting three different surrogates for gasoline FACE A and FACE C fuels, to match the physical and chemical characteristics of these fuels. Good agreement was obtained between the actual fuel and one of the suggested surrogates. For instance, the distillation curve was mimicked by a deviation of approximately 5%. The auto-ignition of gasoline FACE F and its surrogates was investigated experimentally in [11]. The suggested surrogate, which consists of 3 components, showed a good agreement with the full composition of the same fuel.

In a recent study by Elwardany et al. [7], three surrogates consisting of 5, 6 and 7 components were formulated to match the physical characteristics of the gasoline FACE A fuel. The five-component surrogates showed an almost identical droplet surface temperature and lifetime compared to those predicted for the full composition (19 components) of the gasoline FACE A fuel. Twenty diesel fuel surrogates were suggested in [4] to match the thermophysical properties of diesel fuel. Five surrogates were suggested in [8] for gasoline FACE I to match the heating and evaporation of the original fuel. Also, the heating and evaporation of light naphtha and its suggested surrogates were examined in [9]. In the latter study, the formulated surrogates matched the heating and evaporation characteristics of the full compositions. In their recent study, Poulton et al. [17] formulated some surrogates to match the droplet lifetime and surface temperature of kerosene fuel. Their suggested surrogates showed good agreement with the experimental measurements.

There are two types of surrogates, namely, physical and chemical surrogates. Physical surrogates are used to match the processes preceding the onset of combustion (droplet heating and evaporation); while chemical surrogates are used to match the combustion characteristics of fuels [1]. To the best of our knowledge, there has not been any study on formulating surrogates for bio-fossil fuel blends to match both the physical and chemical characteristics of these fuels. In this study, we present a new approach for the formulation of surrogates and examine them for heating and evaporation and some of the main combustion characteristics. A modified version of the Multi-Dimensional Quasi-Discrete Model (MDQDM) (the model was originally introduced in [18] and applied to gasoline, diesel and fuel blends in [19,20]) is used to formulate the physical surrogates of gasoline FACE C, diesel, ethanol/gasoline blends and biodiesel/diesel blends.

2. The model

In 2010, Sazhin [21] introduced a new approach for the simulation of bi-component fuel droplet heating and evaporation, the so-called Discrete Multi-Component Model (DMCM). This model was based on an analytical solution to the transient heat and mass transfer equations [22–24]. The main distinctive feature of the DMCM was that it considered the impacts of species thermal conductivities and diffusivities within the droplet to account for the temperature gradient and transient diffusion of species and recirculation, using effective thermal conductivity and effective diffusivity models [25]. The capability of the DMCM for predicting the droplet heating and evaporation was validated against experimental data for multi-component fuel mixtures [26,27]. The DMCM approach was computationally expensive when used for real applications (i.e., fuels containing 100s of components). In response to this problem, the MDQDM was introduced in [18] to reduce the large number of components with a much smaller number of representative components, the so-called Quasi-Components (QCs). The number of atoms in these QCs is non-integer; hence the name.

The MDQDM uses the same analytical solutions as those used in DMCM for solving the heat and mass transfer equations. The QCs are generated within each hydrocarbon and methyl-ester groups. These components have non-integer carbon numbers (see [20,27] for more details). It is not possible to formulate the physical surrogates of each fuel using these QCs, because they cannot be measured experimentally for validation purposes and cannot be implemented into commercial CFD codes for the

prediction of combustion characteristics, due to the unavailability of their chemical mechanisms. In this paper, we propose a modified version of the MDQDM, described as a 'Complex Fuel Surrogates Model' (CFSM), to generate actual components (with rounding half-up to the nearest integer carbon numbers) and formulate fuel surrogates. The carbon number of each Approximate Discrete Component (ADC) generated by the CFSM can be introduced as:

$$n_{im} = \left\lfloor \frac{\sum_{am}^{bm}(n_{im}\, Y_{im})}{\sum_{am}^{bm} Y_{im}} \right\rceil \quad (1)$$

where m refers to the hydrocarbon group number in the fuel, n is the carbon number of the i^{th} component in group m, Y is the mass fraction of the i^{th} component in group m. In contrast to the original MDQDM (where the QC carbon number is a non-integer value, see Equation (6) in [18]), the nearest integer of the carbon number (ADC) is determined in Equation (1). Also, in contrast to the MDQDM, we use the mass fractions Y_{im} (instead of the molar fractions) to calculate the ADC group averaged carbon number n_{im}. These mass fractions are used to demonstrate the importance of heavy components on the expense of less important (lighter) ones for the prediction of droplet lifetime. For example, alkanes (the heaviest group) make up to 44.53% of diesel mass fractions (only 41.48% diesel molar fractions), which dominates the fuel composition on the expense of lighter components – such as naphthalenes with up to 7.46% mass fractions (9% molar fractions) and alkylbenzenes with up to 13.62% mass fractions (16.75 molar fractions).

The integer ADCs are generated within each group, where am and bm are the start and end counted components of the grouped species, respectively; and am for the second grouped components is $bm_{\text{old}+1}$. For example, a typical diesel fuel has 9 groups of hydrocarbons in which the group of alkanes contains 20 components. To reduce these 20 alkane components to 4 components, each 5 sequential components (sub-group) is grouped to form an ADC. The ADC carbon numbers of each sub-group of alkanes are determined as:

$$\left.\begin{aligned} n_{(1-5)m} &= \left\lfloor \frac{\sum_{i=5}^{i=1}(n_{im}Y_{im})}{\sum_{i=5}^{i=1}Y_{im}} \right\rfloor \\ n_{(6-10)m} &= \left\lfloor \frac{\sum_{i=10}^{i=6}(n_{im}Y_{im})}{\sum_{i=10}^{i=6}Y_{im}} \right\rfloor \\ n_{(11-15)m} &= \left\lfloor \frac{\sum_{i=15}^{i=11}(n_{im}Y_{im})}{\sum_{i=15}^{i=11}Y_{im}} \right\rfloor \\ n_{(16-20)m} &= \left\lfloor \frac{\sum_{i=20}^{i=16}(n_{im}Y_{im})}{\sum_{i=20}^{i=16}Y_{im}} \right\rfloor \end{aligned}\right\} \quad (2)$$

Similarly, the ADC carbon numbers of the other groups are obtained.

3. Diesel fuel surrogates

The diesel fuel surrogates were formulated using the CFSM, and their physical characteristics were compared with those predicted using MDQDM and DMCM. An example of the QCs generated using the MDQDM and the ADCs generated using the CFSM is presented in Table 1, where the 98 components of diesel fuel are replaced by 6 QCs and 6 ADCs.

Table 1. Quasi-Components (QCs) and Approximate Discrete Components (ADCs), representing the groups of species in diesel fuel.

Group	Molar fractions (%)	QCs	Mass fractions (%)	ADCs
n-alkane	41.48	$C_{14.763}H_{31.526}$	44.53	$C_{16}H_{34}$
cycloalkane	15.41	$C_{15.364}H_{30.728}$	17.05	$C_{17}H_{34}$
bi-cycloalkane	7.89	$C_{14.743}H_{27.486}$	8.29	$C_{16}H_{30}$
alkylbenzene	16.75	$C_{11.72}6H_{17.452}$	13.62	$C_{13}H_{20}$
tetraline	9.48	$C_{13.832}H_{19.664}$	9.05	$C_{15}H_{22}$
naphthalene	8.99	$C_{12.392}H_{12.784}$	7.46	$C_{13}H_{14}$

Following [27], a diesel fuel droplet of initial radius $R_{do} = 12.66$ μm and temperature $T_{do} = 360$ K was assumed to be moving at a constant velocity $U_d = 10\ \mathrm{m \cdot s^{-1}}$ in still air. The ambient pressure and temperature were assumed equal to $p_g = 30$ bar and $T_g = 800$ K, respectively. The evolutions of droplet radii predicted using the MDQDM and CFSM were compared to those of the full compositions of diesel fuel using the DMCM, as presented in Figure 1.

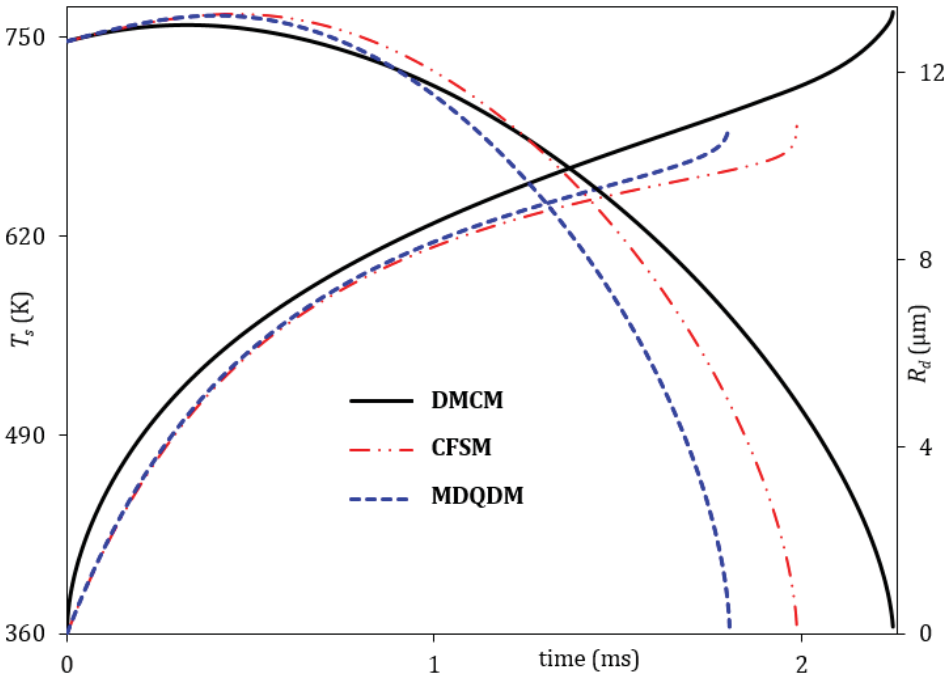

Figure 1. Evolution of droplet surface temperatures and radii predicted for the full compositions of diesel fuel (98 components) using DMCM, 6 approximate discrete components (ADCs) using CFSM, and 6 quasi-components (Qs) using MDQDM. The droplet velocity is 10 $\mathrm{m \cdot s^{-1}}$ in still ambient air of pressure $p_g = 30$ bar and temperature $T_g = 800$ K.

A detailed comparison between the MDQDM and CFSM was made at different time instants. The droplet radii and surface temperatures versus the numbers of Cs/QCs and ADCs were predicted using the MQDQM and CFSM at $t = 0.5$ ms, $t = 1$ ms, $t = 1.5$ ms and $t = 2$ ms, as shown in Figures 2–5.

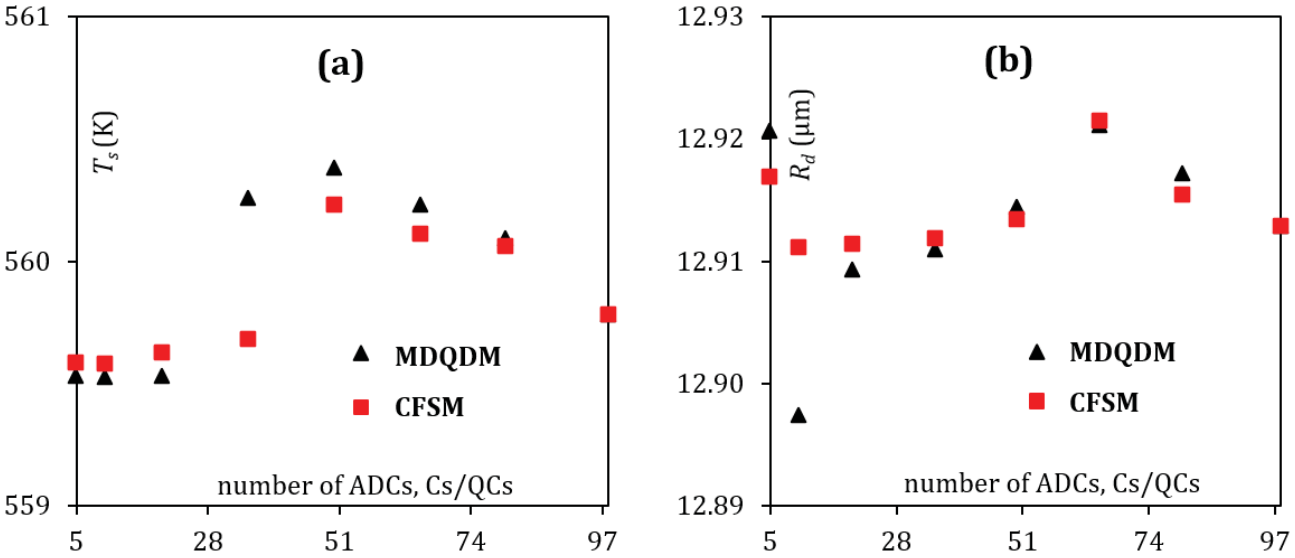

Figure 2. The droplet surface temperatures (a) and radii (b) versus ADCs and Cs/QCs at time instant 0.5 ms, using the same parameters as in Figure 1.

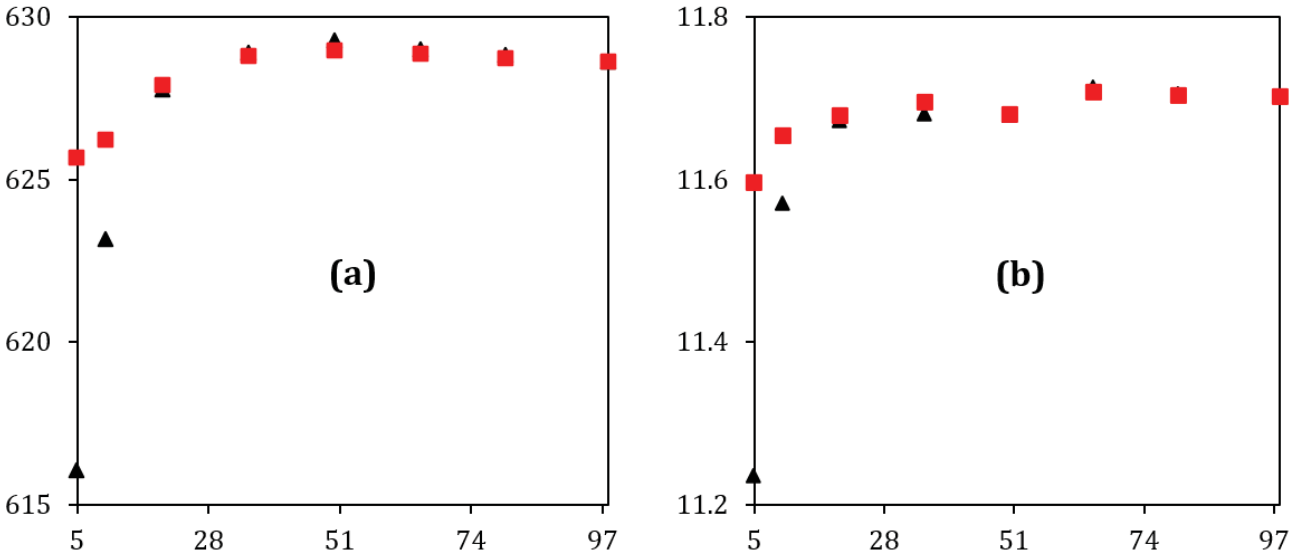

Figure 3. Same as Figure 2, but at time instant 1 ms.

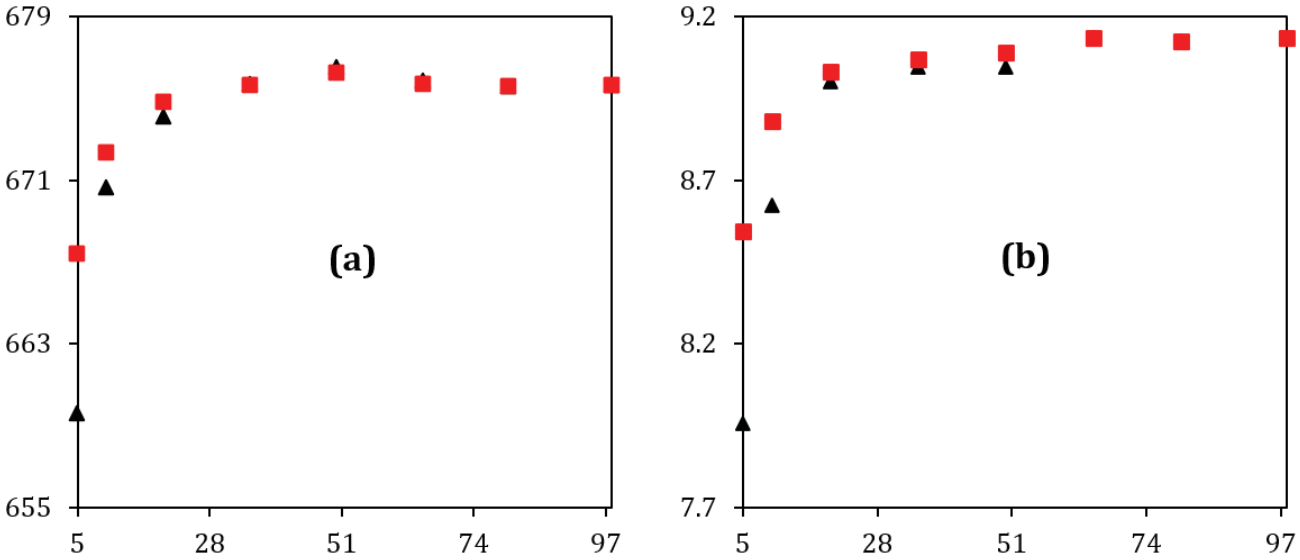

Figure 4. Same as Figures 2-3, but at time instant 1.5 ms.

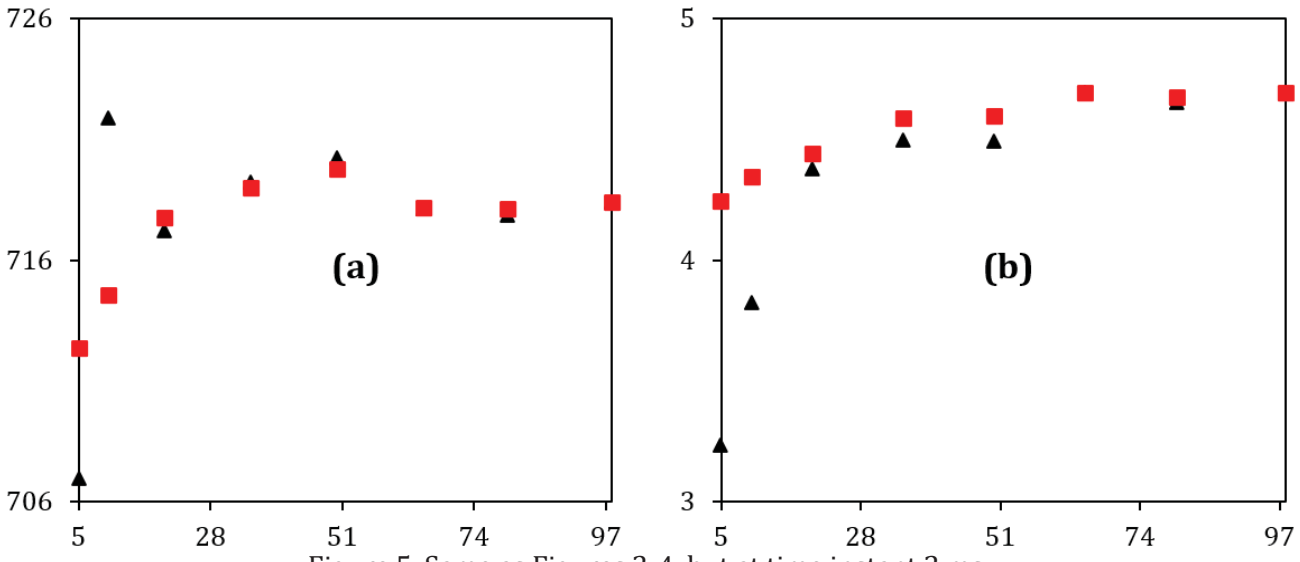

Figure 5. Same as Figures 2-4, but at time instant 2 ms.

As can be seen from Figures 2-5, the predictions of CFSM are generally better than those obtained using the MDQDM especially with the small numbers (≤ 10) of ADCs and Cs/QCs. The predictions of the CFSM for droplet radii and surface temperatures when the full composition of diesel fuel (98 components) is approximated by 10 ADCs are reasonably close to those predicted using the DMCM with up to 4% errors. The results presented in Figures 2-5 confirm the previous trends inferred from Figure 1.

Although the diesel droplet heating and evaporation using the CFSM are verified, the selection of ADCs in this model is still based on trial and error. Hence, this model still requires experienced end-users to run it. The impact of the trial and error on the predicted droplet surface temperatures and radii are noticeable in Figure 2 – where the new approximation of the full composition of diesel fuel with the range 50-75 ADCs overpredicts these results. Some fluctuations are observed in at different time instants (e.g., Figure 5) where those approximations can overpredict or underpredict the results of the 98 components. A universal algorithm is undoubtedly needed for the selection of QCs or ADCs to minimise such uncertainty. In the current work, however, we aim to formulate fuel surrogates that match the real physical and chemical characteristics of their fuels. We have investigated the chemical and physical characteristics of our formulated diesel surrogates using the CFSM (Sur1) and two sets of surrogates from the literature (Sur2 [28] and Sur [29]), in comparison to those of the full composition of diesel fuel in [27]. Table 2 summarises the molar fractions of our formulated surrogates (Sur1) and the other two sets of surrogates (Sur2 and Sur3).

Table 2. The molar fractions of the three surrogates (Sur1, Sur2, and Sur3) of diesel fuel.

Component	Chemical formula	Molar fractions (%)		
		Sur1	Sur2 [28]	Sur3 [29]
n-hexadecane	$C_{16}H_{34}$	42.89	41.3	0.88
iso-cetane	$C_{16}H_{34}$	-	36.8	7.48
n-butylcyclohexane	$C_{10}H_{20}$	-	-	29.66
n-pentylcyclododecane	$C_{17}H_{34}$	16.43	-	-
bi-cyclohexane	$C_{12}H_{24}$	-	-	25.26
bi-cycloocatne	$C_{16}H_{30}$	7.89	-	-
toluene	C_7H_8	-	-	10.94
heptylbenzene	$C_{13}H_{20}$	13.12	-	-
decalin	$C_{10}H_{18}$	-	-	25.78
1-dimethyl-4-iso-propyltetralin	$C_{15}H_{22}$	8.72	-	-
naphthalene	$C_{11}H_{10}$	-	21.9	-
1-methyl-2-ethyl-naphthalene	$C_{13}H_{14}$	10.95	-	-

The diesel fuel droplet lifetimes were investigated for the full composition of fuel, using the DMCM and the three surrogates (Sur1, Sur2 and Sur3) the evolutions of which are illustrated in Figure 6. The droplet initial temperature was assumed equal to $T_{do} = 296$ K.

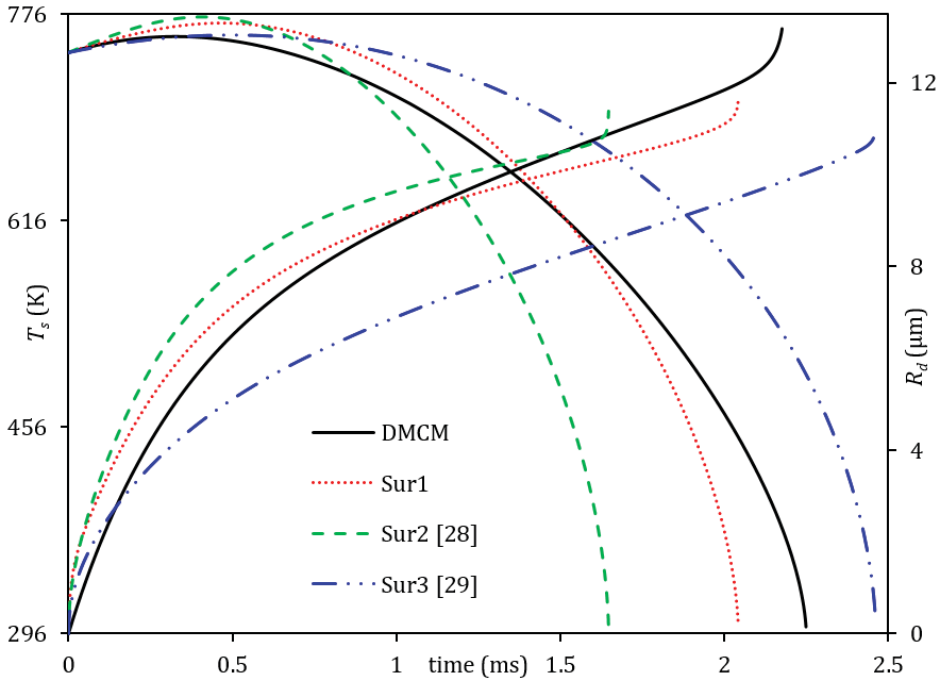

Figure 6. Evolutions of droplet surface temperatures and radii for the full compositions of diesel fuel and its 3 surrogates (Sur1, Sur2 and Sur3), using the same parameters as in Figures 1-5 but for droplet initial temperature equal to $T_{do} = 296$ K.

In Figure 6, the evolutions of droplet radii of Sur1 are of reasonably close with those predicted for the full compositions of diesel, where it underpredicts the droplet's lifetime by only 7.2%. The predictions of Sur2 (inferred from [28]) and Sur3 (inferred from [29]), however, can expose the predictions of droplet lifetimes to errors up to 26.8% and 8.3%, respectively. Also, the droplet surface temperatures are underpredicted by 7.3%, 8.4% and 9.9% using Sur1, Sur2 and Sur3 respectively. These errors are estimated in comparison to the same values of the full composition of diesel fuel using the DMCM.

To further understand the suitability of the suggested surrogates to represent diesel fuel, the Cetane Number (CN) was calculated for these surrogates. In the original composition of diesel fuel presented in [18], n-alkanes and iso-alkanes were merged into one group due to their similar thermodynamic and transport properties. For the calculation of CN, however, these two groups were treated individually in our analysis, due to their different CN values with various component structures – normal (straight chains) or isomers (branched chains) [30]. The viscosities of the two suggested surrogates were also compared to the full compositions of diesel fuel. The viscosity is an important factor for the atomisation

and combustion processes [31,32]. It was predicted using the UNIFAC–VISCO method [33]. The predictions of the CNs and the viscosities of our formulated surrogates using the CFSM (Sur1) and the other two sets of surrogates (Sur2 and Sur3) were compared to those calculated for the full compositions of diesel fuel as shown in Table 3.

Table 3. The CNs and viscosities (in cP) of diesel fuel and its three surrogates (Sur1, Sur2 and Sur3).

Fuel	CN	Error (%)	Viscosity	Error (%)
diesel	54.5	-	4.516	-
Sur1	53.3	2.2	4.442	1.6
Sur2 [28]	39.8	27.0	4.483	0.8
Sur3 [29]	60.1	10.3	3.35	26.2

As can be seen from Table 3, Sur1 mimics the CN of diesel fuel with an error of less than 3%. Also, Sur1 and Sur2 match the viscosity of the full composition of diesel fuel, but with errors of up to 1.6% and 0.8%, respectively. As can be seen from these results (Figure 6 and Table 3), Sur2 model predictions are exposed to significant errors, beyond the acceptable limit. This is ascribed to the fact that Sur2 (composed of 3 components) is dominated by alkanes (78.1%, as shown in Table 2), ignoring the fair contributions of other hydrocarbons. Considering the importance of physical and chemical features of fuel surrogates (droplet's lifetime and temperature, CN and viscosity), Sur1 is relatively the best surrogate group to represent diesel fuel, compared with Sur 2 and Sur3 surrogates.

4. Gasoline fuel surrogates

The droplet surface temperature and lifetime for the full composition of gasoline FACE C were predicted in [19,26], assuming Raoult's law was valid. In our previous study [34], the impact of activity coefficient on the vapour-liquid equilibrium for this fuel was accounted for. In this section, we present the comparison of the physical and chemical features of the full composition of fuel obtained from [19,26], our formulated surrogates using the CFSM (Sur4), and the two surrogates (Sur5 and Sur6) inferred from [5,6]. Table 4 illustrates the molar fraction of the three surrogates.

Table 4. The molar fractions of the three surrogates (Sur4, Sur5 and Sur6) of gasoline fuel.

Component	Molar fractions (%)		
	Sur4	Sur5 [5]	Sur6 [6]
n-butane	-	17.0	18.4

n-pentane	29.18	-	-
n-heptane	-	11.0	12.5
n-undecane	0. 03	-	-
iso-pentane	10.74	8.0	5.0
iso-heptane	-	5.0	4.7
iso-octane	55.23	56.0	54.6
iso-decane	0.48	-	-
toluene	-	3.0	4.8
iso-propylbenzene	4.34	-	-

Initially, we predicted the droplet surface temperatures and lifetimes using DMCM. Following [26,34], the initial droplet radius was taken as equal to $R_{do} = 12$ μm, the droplet was at initial temperature $T_{do} = 296$ K and moving at a constant velocity $U_d = 24$ m · s^{-1}. The ambient gas (still air) pressure and temperature were assumed constant and equal to $p_g = 9$ bar and $T_g = 545$ K, respectively. The predicted evolutions of droplet radii and surface temperatures for the full compositions and the three surrogates are presented in Figure 7.

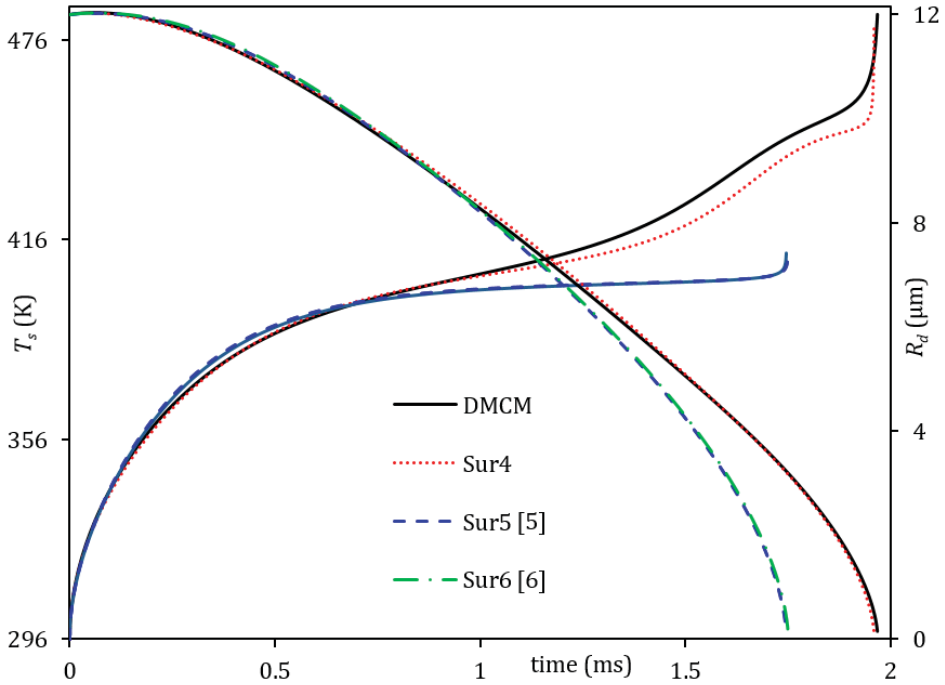

Figure 7. Evolutions of droplet radii and surface temperatures for the full compositions of gasoline and its 3 suggested surrogates: Sur4 (derived using the CFSM), Sur5 (inferred from [5]) and Sur6 (inferred from [6]). The droplet, with initial temperature $T_{do} = 296$ K, was moving at $U_d = 24$ m · s^{-1} in still ambient air of pressure $p_g = 9$ bar and temperature $T_g = 545$ K.

As shown in Figure 7, the predictions of Sur4 droplet surface temperatures and radii, using the CFSM, are only 0.71% and 0.41%, respectively, less than those predicted for the full composition of the same fuel using the DMCM. At the same time, the use of the Sur5 and Sur6 surrogates underpredicts the

droplet lifetimes and surface temperatures by up to 15% and 11.3%, respectively. The densities and vapour pressures of the three fuel surrogates (Sur4, Sur5 and Sur6) and the full composition were calculated at the same input parameters and transient conditions of the droplet. The density of each component was predicted using the data inferred from [35]. The linear blending of volume fractions was used to make up the density of the mixture. The vapour pressure was calculated using the set of expressions provided in [33] for each component. The modified Raoult's law, using the UNIFAC model (see [34] for details), was used to determine the partial vapour pressure of each component. The predicted values of densities and vapour pressures for the full composition of fuel and the three fuel surrogates (Sur4, Sur5 and Sur6) are presented in Table 5.

Table 5. The calculated vapour pressures (in kPa) and densities (in $\mathrm{kg \cdot m^{-3}}$) for gasoline fuel and its surrogates (Sur4, Sur5 and Sur6) at 296 K.

Fuel	Vapour pressure	Error (%)	Density	Error (%)
gasoline	34.25	-	682.3	-
Sur4	35.77	4.4	680.8	0.22
Sur5 [5]	54.49	59.1	680.3	0.29
Sur6 [6]	52.41	53.0	683.3	0.15

As can be read from Table 5, the densities of all three surrogates are found to be in close agreement to that predicted for the full composition of gasoline fuel. However, the vapour pressures of the two surrogates, Sur5 and Sur6 (inferred from [5,6]), are found to be significantly different from those calculated for the full composition of gasoline fuel, showing errors of up to 59.1% and 53%, respectively. These large errors produced by Sur5 and Sur 6 surrogates were expected, because these surrogates were originally developed to match some ignition related factors (mainly, H/C, MW and RON) ignoring the physical processes (e.g., droplet lifetime and vapour pressure). We predicted these characteristics using Sur4, which provided only up to 4.4% errors, compared to the predictions of DCM.

The H/C ratio, MW and RON were compared to those of the full composition of gasoline FACE C. According to [36], the flame speed and the diffusivity of the real fuel can be matched using the suggested surrogates when the H/C ratio and the MWs are matched. Also, the ignition time delays of the fuel and its surrogates can be matched when their RONs are in good agreement [5]. The H/C ratios were predicted for the suggested surrogates using the following relationship [6]:

$$\frac{H}{C} = \frac{\sum_i^n X_i(N_{Hi})}{\sum_i^n X_i(N_{Ci})}, \quad (3)$$

where X_i, N_{Ci}, H_{Ci} are the molar fraction, number of carbon atoms, and number of hydrogen atoms respectively, of their i^{th} component. The RON of Sur4 was predicted using the following relationship [37]:

$$\mathrm{RON} = \frac{\sum_i v_i \beta_i \mathrm{ON_i}}{\sum_i v_i \beta_i}, \quad (4)$$

where v_i is the volume fraction of component i, β_i is a parameter value for each hydrocarbon group and $\mathrm{ON_i}$ is the octane number of component i. Equation 4 can be used for the predictions of RON and MON by using the appropriate β_i. The MW was calculated using the linear blending of the molar fractions. The values of RON, MW and the H/C ratio of the full composition fuel and the three surrogates are shown in Table 6. It should be emphasised that the RON, predicted in [5,6] for Sur5 and Sur6, were based on the linear molar blending rule and not on detailed hydrocarbon groups. As can be seen from this table, our suggested surrogates match the three aforesaid properties with negligible deviation compared to the full composition of FACE C gasoline fuel.

Table 6. The RONs, H/C ratios and MWs (in $\mathrm{g \cdot mole^{-1}}$) of gasoline fuel and its surrogates.

Fuel	RON	H/C	MW
gasoline	84.7	2.27	97.2
Sur4	85.8	2.24	97.8
Sur5 [5]	85.3	2.25	98.4
Sur6 [6]	85.3	2.23	98.1

5. Blended ethanol-gasoline surrogates

The predictions of the droplet heating and evaporation of biodiesel, ethanol, ethanol/gasoline blends and biodiesel/diesel blends were investigated in [20,26,38–42]. Due to the interest in increasing the fraction of biofuels in the baseline fuel and to comply with some of the recent governmental regulations (for instance, the UK Department for Transport announced in April 2018 that the government was aiming to double the use of biofuel from its current 4.9% to 9.75% by 2020), the formulation of bio-fossil fuel blend surrogates is essential to study the feasibility of increasing the biofuel fractions. In a recent study, the isoamyl alcohol proved to be a suitable fuel to be blended with gasoline without any engine modifications [43]. Therefore, we have tried to formulate surrogates for ethanol/gasoline blends.

The ethanol/gasoline fuel surrogates were generated using the input parameters and ambient conditions described in section 4. The UNIFAC model was implemented for all functional groups in this section (without any approximation) due to the significant non-ideality of ethanol/gasoline blends. The impact of ethanol addition on droplet lifetime and surface temperature was presented in [26,34]. In this study, the impact of ethanol on the RON and the densities was investigated and compared to those of pure gasoline. In addition, the predictions of all the aforementioned characteristics were predicted by the suggested fuel surrogates and compared to the full composition of fuel. The RONs and the densities of different fractions of ethanol/gasoline blends are shown in Table 7 (EX is referred to X vol. % ethanol and (100-X) vol. % gasoline).

Table 7. The RONs and densities (in $kg \cdot m^{-3}$) of ethanol/gasoline fuel blends.

Fuel	RON	Density
gasoline	85.8	680.4
E5	87.7	685.7
E20	92.7	701.7
E50	100	773.8
E85	106	770.1
E100	108	787.2

Results indicate that the addition of ethanol can be sacrificed in gasoline engines by up to 20% due to the minor deviations in RON and density (which were 8% and 3%, respectively) compared to pure gasoline. According to our findings in [34] and in the current work, ethanol can be blended with gasoline by up to 20% without any engine modifications. Based on these findings, the E20 was used for the surrogate formulation of the ethanol/gasoline blend. The molar fractions of our suggested surrogate, using the CFSM and the surrogates suggested in [44], are shown in Table 8.

Table 8. The molar fractions of E20 surrogates (Sur7 and Sur8).

Component	Molar fractions (%)	
	Sur7	Sur8 [44]
n-hexane	18.13	-
n-heptane	-	11.82
iso-pentane	6.64	-
iso-octane	31.17	25.28
iso-decane	2.83	-

toluene	-	25.81
iso-propylbenzene	3.1	-
ethanol	38.13	37.08

The evolutions of the droplet radii and surface temperatures predicted by our formulated fuel surrogates (Sur7), the surrogates suggested in the literature (Sur8 [44]) and the full composition of the E20 blend, are shown in Figure 8.

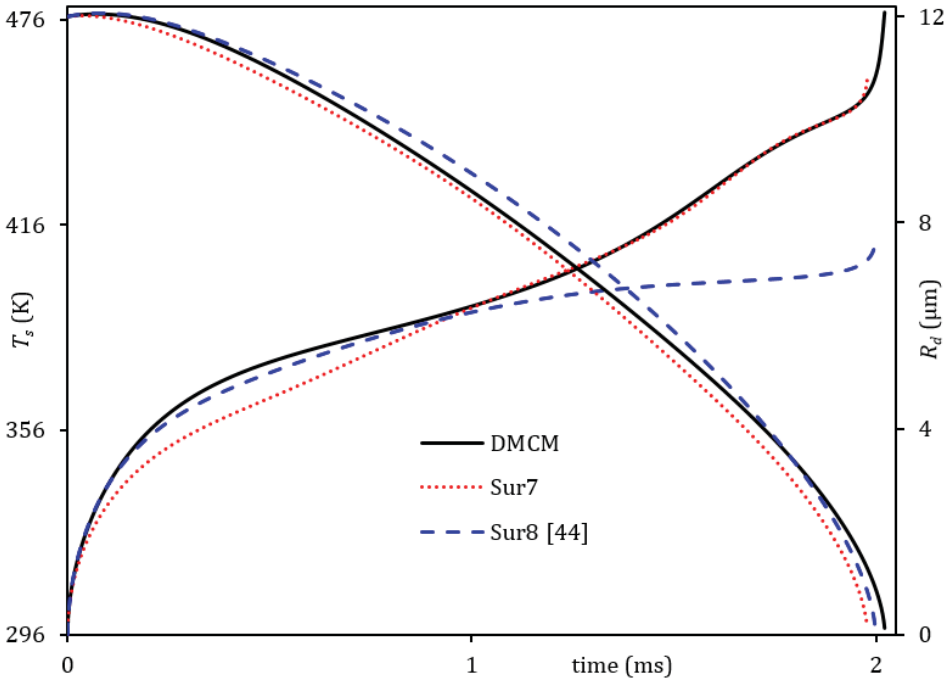

Figure 8. Evolution of the droplet radii and surface temperatures for the full compositions of E20 and the two surrogates (Sur7 and Sur8).

The predictions reveal that our surrogates (Sur7) is in a good agreement with the full composition of E20. The predicted errors in droplet lifetime and surface temperature are up to 2.1% and 4%, respectively, compared to the same results predicted using the DMCM. Similarly, a negligible deviation in droplet lifetime, compared to the full composition of gasoline, is predicted for Sur8 (the surrogates inferred from [44]). However, using Sur8 shows a significant deviation in the droplet surface temperature with up to 14%. The RON, H/C and MW were studied to examine the ability of the two surrogates by means of fuel representation, as shown in Table 9. The RON, H/C and MW predicted by the two surrogates show a good agreement with those predicted by the full composition of gasoline fuel.

Table 9. The RONs, H/C ratios and MWs (in $g \cdot mole^{-1}$) of E20 fuel blends and its surrogates.

Fuel	RON	H/C	MW
E20	92.5	2.23	78.22
Sur7	95.3	2.24	79.54

Sur8 [44]	96.4	2.25	81.59

To further verify the CFSM ability to generate fuel surrogates, the E50 and E85 fuel blends of ethanol/gasoline are examined. The molar fractions of the formulated surrogates of these two blends (Sur9 for E50 and Sur10 for E85) are provided in Table 10.

Table 10. The molar fractions of Sur9 (surrogates of E50) and Sur10 (surrogates of E85).

Component	Molar fractions (%)	
	Sur9 (E50)	Sur10 (E85)
n-hexane	8.54	1.98
iso-pentane	3.09	0.72
iso-octane	14.54	3.37
iso-decane	1.32	0.31
iso-propylbenzene	1.45	0.33
Ethanol	71.15	93.29

The evolutions of droplet surface temperatures and lifetimes of the original composition of E50 and E85 fuel blends and their surrogates Sur9 and Sur10, respectively, are presented in Figure 9. Also, the RONs, H/C ratios and MWs of these fuel blends and their surrogates (Sur9 and Sur10) are presented in Table 11. As evident from these figure and table, the formulated surrogates for both E50 and E85 blends capture the original characteristics of the full compositions of both fuel blends.

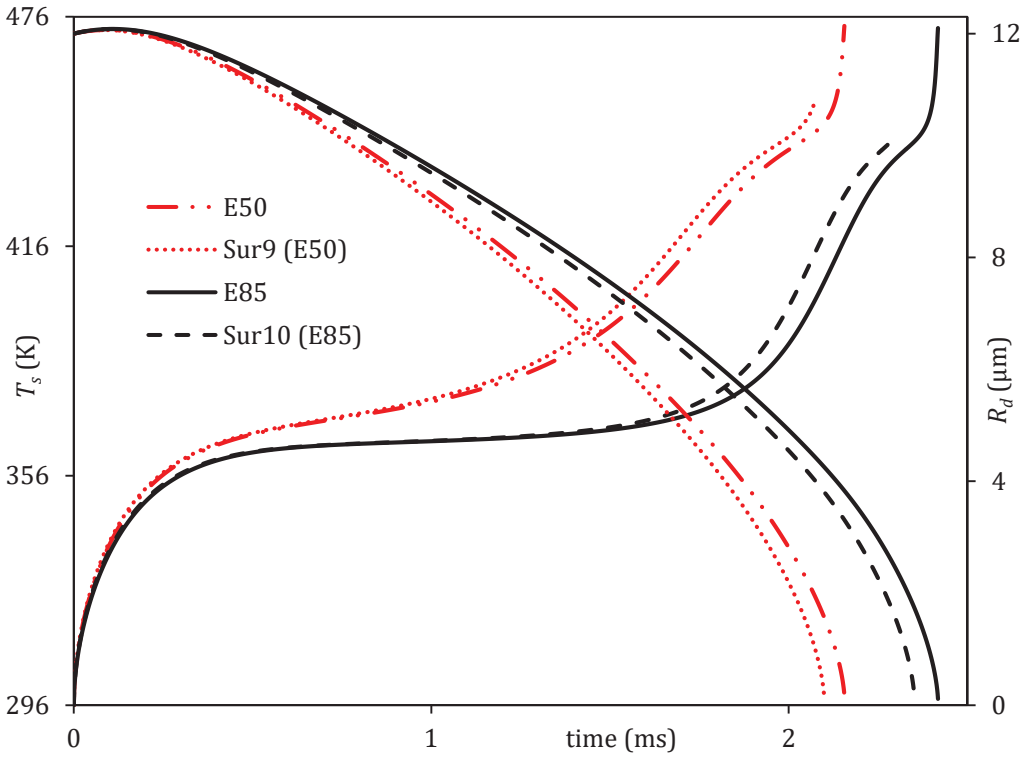

Figure 9. Evolutions of the droplet radii and surface temperatures for the full compositions of E50 and E85 and their two surrogates (Sur9 and Sur10).

Table 11. The RONs, H/C ratios and MWs (in $g \cdot mole^{-1}$) of E50 and E85 fuel blends and their surrogates.

Fuel	RON	H/C	MW
E50	100.1	2.55	61.03
Sur9 (E50)	102.7	2.58	61.4
E85	106	2.85	49.55
Sur10 (E85)	107	2.85	49.61

6. Blended biodiesel-diesel surrogates

The feasibility of adding biodiesel fuel to diesel at different fractions has been highlighted in many studies (e.g., see [20]). Adding biodiesel to diesel can lead to a noticeable reduction in CO and smoke emissions [45,46]. According to the latest renewable fuel statistics report by the UK Department for Transport, 80% of the biodiesel produced in the UK was from used cooking oil, which accounts for around 115 million litres [47]. Therefore, biodiesel/diesel surrogates are commonly based on the blend of waste cooking oil biodiesel and diesel [48]. To the best of our knowledge, there is insufficient literature about the surrogates of Waste Cooking Oil (WCO) and its diesel blends. The impact of biodiesel addition on droplet lifetime and surface temperature was presented in [39]. In the current study, the impact of biodiesel on the CN was investigated and compared to that of pure diesel. The CN, predicted by different WCO biodiesel/diesel blends using the expression provided in our previous work [30]

which is based on the linear blending of volume fractions, is shown in Table 12. The original composition of WCO biodiesel fuel was inferred from [49].

Table 12. The CNs of biodiesel/diesel fuel blends.

Fuel	CN
diesel	54.5
B5	54.8
B10	55.1
B20	55.8
B50	57.7
B100	60.9

Following our recent finding in [39] and Table 12, biodiesel can be blended with diesel by up to 10% without a need for engine modification. In this section, we have used the same ambient conditions and input parameters as in Section 3 to generate surrogates of B10 (10% vol. biodiesel and 90% vol. diesel fuel blend), B20 and B50. We have examined the major physical and chemical fuel characteristics of the full compositions of B10, B20 and B50, compared with their formulated surrogates, Sur11, Sur12 and Sur13, respectively, using the CFSM. The molar fractions of these surrogates are presented in Table 13.

Table 13. The molar fractions of the B10, B20 and B50 surrogates (Sur11, Sur12 and Sur13).

Component	Chemical formula	Molar fractions (%)		
		Sur11 (B10)	Sur12 (B20)	Sur13 (B50)
n-hexadecane	$C_{16}H_{34}$	38.60	34.31	21.44
n-pentylcyclododecane	$C_{17}H_{34}$	14.79	13.15	8.22
bi-cycloocatne	$C_{16}H_{30}$	7.09	6.30	3.94
heptylbenzene	$C_{13}H_{20}$	11.81	10.49	6.56
1-dimethyl-4-isopropyltetralin	$C_{15}H_{22}$	7.85	6.97	4.36
1-methyl-2-ethylnaphthalene	$C_{13}H_{14}$	9.86	8.78	5.48
1-methyl-oleate	$C_{19}H_{36}O_2$	5.85	11.71	29.25
1-methyl-linoleate	$C_{19}H_{34}O_2$	4.15	8.29	20.75

The WCO fuel consists of 8 saturated components (making 24.1% of the fuel), 4 unsaturated components with one double bond (making 44.4% of the fuel) and 2 unsaturated components with two double bonds (making 31.5% of the fuel). Therefore, the dominant two groups are those with unsaturated methyl esters; hence the two dominant unsaturated components 1-methyl-oleate and 1-methyl-linoleate were chosen to represent WCO in B10, B20 and B50 fuel blend surrogates (Sur11, Sur12 and Sur13). The droplet radii and surface temperatures are predicted for Sur11, Sur12 and Sur13, using the CFSM, and compared with those of the full compositions of B10, B20 and B50 blends, using the DMCM, as shown in

Figure 10. As can be seen from this figure, the droplet lifetime and temperatures of the fuel surrogates are in good agreements with those predicted for the full compositions of their fuels. For instance, the surrogate droplet lifetimes and temperatures are underpredicted by up to 7.16% and 4.51%, compared with the full composition of B10. These underpredictions can be tolerated in some engineering applications.

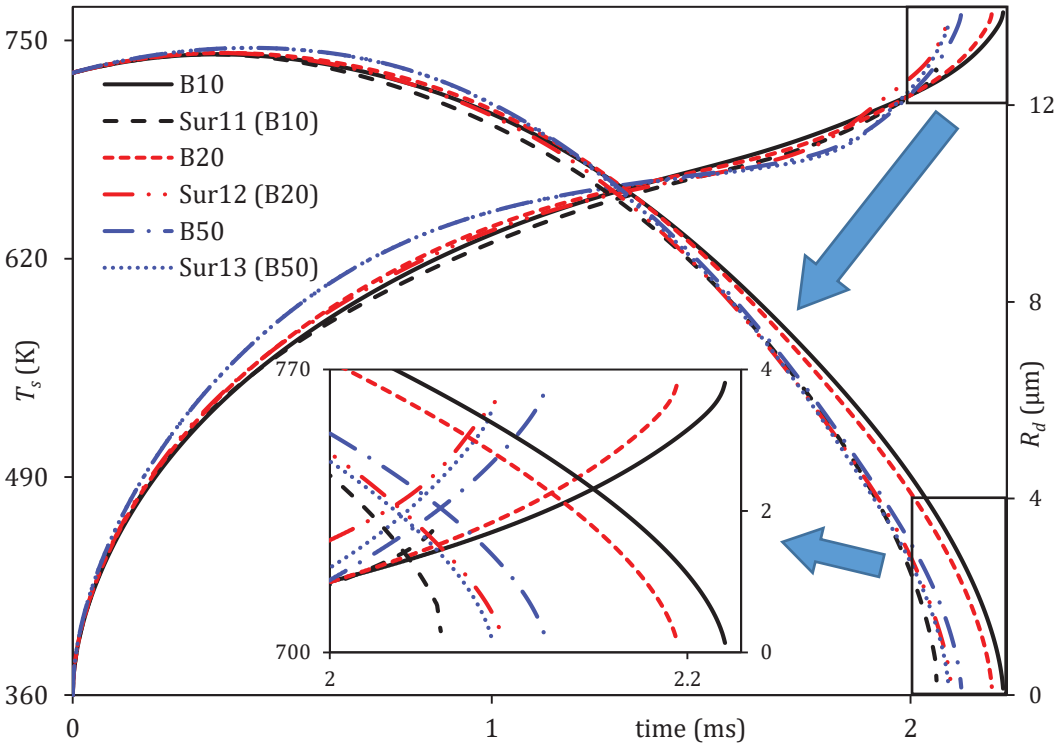

Figure 10. Evolutions of droplet radii and surface temperatures for the full compositions of B10, B20 and B50 and their suggested surrogates.

The CN (predicted by the surrogate) is also compared to the full composition of B10. The CN of Sur11 (53.9) shows a reasonable agreement with that of the full composition of B10 (55.1). Similarly, the CN predicted by the formulated surrogates of B20 (Sur12) and B50 (Sur13) fuel blends show very good agreements with those predicted for the full compositions of the same fuel blends. We can conclude that the droplet lifetimes and surface temperatures and CN of our formulated surrogates (Sur11, Sur12 and Sur13) for the B10, B20 and B50 fuel blends match the full composition characteristics of these fuels.

7. Conclusion

The Multi-Dimensional Quasi-Discrete Model (MDQDM), based on the advanced Discrete Multi-Component Model (DMCM), was modified to formulate fuel surrogates using a new approach, described as a 'Complex Fuel Surrogates Model' (CFSM). The CFSM was verified against the DMCM, in application

to the full compositions of gasoline and diesel fuels and their ethanol/gasoline and biodiesel/diesel blends. The main purpose of this work was to formulate accurate fuel surrogates and broaden the usefulness of the model for future implementation into commercial CFD codes and experimental validations. The physical and chemical properties of the formulated surrogates (Sur1 for diesel, Sur4 for gasoline, Sur7 for E20, Sur9 for E50, Sur10 for E85, Sur11 for B10, Sur12 for B20, Sur13 for B50) were compared to the full compositions of each fuel.

Our proposed surrogates were verified physically, in terms of their evolutions of droplet radii and surface temperatures, and chemically, in terms of their chemical properties (e.g., H/C, research octane numbers for gasoline and ethanol/gasoline fuels, and cetane numbers for diesel and biodiesel/diesel fuels). The same physical and chemical verifications were applied to the fuel surrogates recommended in literature (noting that the surrogates of biodiesel/diesel blend have not been presented anywhere in literature to the best of our knowledge). The chemical and physical behaviours of our four surrogates were in reasonably close agreements with those predicted for the full compositions of their fuels, exceeding the relative predictions of these fuels provided by the surrogates suggested in literature. For example, in the case of gasoline fuel the literature alternatives to Sur4 exposed the predicted droplet lifetimes to errors of up to 26.8% and the predicted vapour pressure to errors of up to 59.1%. The usefulness of the introduced CFSM was verified for the formulation of surrogates in application to a broad range of fuel compositions.

Nomenclature

Abbreviations

ADCs	approximate discrete components
B#	#% volume biodiesel/diesel fraction
CFD	computational fluid dynamics
CFSM	complex fuel surrogate model
CN	cetane number
DMCM	discrete multi-component model
E#	#% volume ethanol/gasoline fraction
FACE	fuel used in advanced combustion engines
H/C	hydrogen/carbon
MDQDM	multi-dimensional quasi-discrete model
MON	motor octane number
MW	molar weight
ON	octane number
QCs	quasi-components
RON	research octane number

Sur#	surrogate number
UNIFAC	universal quasi-chemical functional–group activity coefficient
WCO	waste cooking oil

Symbols

m	hydrocarbon group number
n	carbon number
N	number of atoms
p	pressure
R	radius
t	time
T	temperature
U	velocity
v	volume fraction
x	molar fraction
y	mass fraction

Greek symbol

β	parameter value for octane number

Subscripts

C	carbon
d	droplet
g	gas
H	hydrogen
s	droplet surface

Acknowledgment

The authors are grateful to the Institute for Future Transport and Cities, Coventry University (Project Ref. ECR019) for providing financial support for the work on this project.

References

[1] Sarathy SM, Farooq A, Kalghatgi GT. Recent progress in gasoline surrogate fuels. Progress in Energy and Combustion Science 2018;65:67–108. https://doi.org/10.1016/j.pecs.2017.09.004.

[2] Pitz WJ, Mueller ChJ. Recent progress in the development of diesel surrogate fuels. Progress in Energy and Combustion Science 2011;37:330–50. https://doi.org/10.1016/j.pecs.2010.06.004.

[3] Mati K, Ristori A, Gaïl S, Pengloan G, Dagaut P. The oxidation of a diesel fuel at 1–10atm: Experimental study in a JSR and detailed chemical kinetic modeling. Proceedings of the Combustion Institute 2007;31:2939–46. https://doi.org/10.1016/j.proci.2006.07.073.

[4] Lin R, Tavlarides LL. Thermophysical properties needed for the development of the supercritical diesel combustion technology: Evaluation of diesel fuel surrogate models. The Journal of Supercritical Fluids 2012;71:136–46. https://doi.org/10.1016/j.supflu.2012.08.003.

[5] Sarathy SM, Kukkadapu G, Mehl M, Wang W, Javed T, Park S, et al. Ignition of alkane-rich FACE gasoline fuels and their surrogate mixtures. Proceedings of the Combustion Institute 2015;35:249–57. https://doi.org/10.1016/j.proci.2014.05.122.

[6] Ahmed A, Goteng G, Shankar VSB, Al-Qurashi K, Roberts WL, Sarathy SM. A computational methodology for formulating gasoline surrogate fuels with accurate physical and chemical kinetic properties. Fuel 2015;143:290–300. https://doi.org/10.1016/j.fuel.2014.11.022.

[7] Elwardany AE, Sazhin SS, Im HG. A new formulation of physical surrogates of FACE A gasoline fuel based on heating and evaporation characteristics. Fuel 2016;176:56–62. https://doi.org/10.1016/j.fuel.2016.02.041.

[8] Elwardany A, Badra J, Sim J, Khurshid M, Sarathy M, Im H. Modeling of heating and evaporation of FACE I gasoline fuel and its surrogates, 2016, SAE 2016 World Congress and Exhibition. https://doi.org/10.4271/2016-01-0878.

[9] Kabil I, Sim J, Badra JA, Eldrainy Y, Abdelghaffar W, Mubarak Ali MJ, et al. A surrogate fuel formulation to characterize heating and evaporation of light naphtha droplets. Combustion Science and Technology 2018;190:1218–31. https://doi.org/10.1080/00102202.2018.1444037.
[10] Pati A, Gierth S, Haspel P, Hasse C, Munier J. Strategies to define surrogate fuels for the description of the multicomponent evaporation behavior of hydrocarbon fuels, 2018. https://doi.org/10.4271/2018-01-1692.
[11] Kang D, Fridlyand A, Goldsborough SS, Wagnon SW, Mehl M, Pitz WJ, et al. Auto-ignition study of FACE gasoline and its surrogates at advanced IC engine conditions. Proceedings of the Combustion Institute 2018. https://doi.org/10.1016/j.proci.2018.08.053.
[12] Qian Y, Yu L, Li Z, Zhang Y, Xu L, Zhou Q, et al. A new methodology for diesel surrogate fuel formulation: Bridging fuel fundamental properties and real engine combustion characteristics. Energy 2018;148:424–47. https://doi.org/10.1016/j.energy.2018.01.181.
[13] Sazhina EM, Sazhin SS, Heikal MR, Marooney CJ. The Shell autoignition model: applications to gasoline and diesel fuels. Fuel 1999;78:389–401. https://doi.org/10.1016/S0016-2361(98)00167-7.
[14] Sazhina EM, Sazhin SS, Heikal MR, Babushok VI, Johns RJR. A detailed modelling of the spray ignition process in diesel engines. Combustion Science and Technology 2000;160:317–44. https://doi.org/10.1080/00102200008935806.
[15] Sileghem L, Alekseev VA, Vancoillie J, Van Geem KM, Nilsson EJK, Verhelst S, et al. Laminar burning velocity of gasoline and the gasoline surrogate components iso-octane, n-heptane and toluene. Fuel 2013;112:355–65. https://doi.org/10.1016/j.fuel.2013.05.049.
[16] Davidson DF, Shao JK, Choudhary R, Mehl M, Obrecht N, Hanson RK. Ignition delay time measurements and modeling for gasoline at very high pressures. Proceedings of the Combustion Institute 2018. https://doi.org/10.1016/j.proci.2018.08.032.
[17] Poulton L, Rybdylova O, Zubrilin IA, Matveev SG, Gurakov NI, Al Qubeissi M, et al. Modelling of multi-component kerosene and surrogate fuel droplet heating and evaporation characteristics: A comparative analysis. Fuel 2020;269:117115. https://doi.org/10.1016/j.fuel.2020.117115.
[18] Sazhin SS, Al Qubeissi M, Nasiri R, Gun'ko VM, Elwardany AE, Lemoine F, et al. A multi-dimensional quasi-discrete model for the analysis of Diesel fuel droplet heating and evaporation. Fuel 2014;129:238–66. https://doi.org/10.1016/j.fuel.2014.03.028.
[19] Al Qubeissi M, Sazhin SS, Turner J, Begg S, Crua C, Heikal MR. Modelling of gasoline fuel droplets heating and evaporation. Fuel 2015;159:373–84. https://doi.org/10.1016/j.fuel.2015.06.028.
[20] Al Qubeissi M, Sazhin SS, Elwardany AE. Modelling of blended Diesel and biodiesel fuel droplet heating and evaporation. Fuel 2017;187:349–55. https://doi.org/10.1016/j.fuel.2016.09.060.
[21] Sazhin SS, Elwardany A, Krutitskii PA, Castanet G, Lemoine F, Sazhina EM, et al. A simplified model for bi-component droplet heating and evaporation. International Journal of Heat and Mass Transfer 2010;53:4495–505. https://doi.org/10.1016/j.ijheatmasstransfer.2010.06.044.
[22] Sazhin SS. Advanced models of fuel droplet heating and evaporation. Progress in Energy and Combustion Science 2006;32:162–214. https://doi.org/10.1016/j.pecs.2005.11.001.
[23] Sazhin SS. Droplets and Sprays. London: Springer; 2014.
[24] Sazhin SS. Modelling of fuel droplet heating and evaporation: Recent results and unsolved problems. Fuel 2017;196:69–101. https://doi.org/10.1016/j.fuel.2017.01.048.
[25] Abramzon B, Sirignano WA. Droplet vaporization model for spray combustion calculations. International Journal of Heat and Mass Transfer 1989;32:1605–18. https://doi.org/10.1016/0017-9310(89)90043-4.
[26] Al Qubeissi M, Al-Esawi N, Sazhin SS, Ghaleeh M. Ethanol/gasoline droplet heating and evaporation: Effects of fuel blends and ambient conditions. Energy & Fuels 2018;32:6498–506. https://doi.org/10.1021/acs.energyfuels.8b00366.
[27] Al-Esawi N, Al Qubeissi M, Whitaker R, Sazhin SS. Blended E85–diesel fuel droplet heating and evaporation. Energy & Fuels 2019;33:2477–88. https://doi.org/10.1021/acs.energyfuels.8b03014.
[28] Yu L, Mao Y, Li A, Wang S, Qiu Y, Qian Y, et al. Experimental and modeling validation of a large diesel surrogate: Autoignition in heated rapid compression machine and oxidation in flow reactor. Combustion and Flame 2019;202:195–207. https://doi.org/10.1016/j.combustflame.2019.01.012.
[29] Huang Z, Xia J, Ju D, Lu X, Han D, Qiao X, et al. A six-component surrogate of diesel from direct coal liquefaction for spray analysis. Fuel 2018;234:1259–68. https://doi.org/10.1016/j.fuel.2018.07.138.
[30] Al-Esawi N, Al Qubeissi M, Kolodnytska R. The Impact of biodiesel fuel on ethanol/diesel blends. Energies 2019;12:1804. https://doi.org/10.3390/en12091804.
[31] Tse H, Leung CW, Cheung CS. Investigation on the combustion characteristics and particulate emissions from a diesel engine fueled with diesel-biodiesel-ethanol blends. Energy 2015;83:343–50. https://doi.org/10.1016/j.energy.2015.02.030.

[32] Labeckas G, Slavinskas S, Mažeika M. The effect of ethanol–diesel–biodiesel blends on combustion, performance and emissions of a direct injection diesel engine. Energy Conversion and Management 2014;79:698–720. https://doi.org/10.1016/j.enconman.2013.12.064.
[33] Poling BE, Prausnitz JM, O'Connell JP. The Properties of Gases and Liquids. New York: McGraw-Hill; 2001.
[34] Al-Esawi N, Al Qubeissi M, Sazhin SS, Whitaker R. The impacts of the activity coefficient on heating and evaporation of ethanol/gasoline fuel blends. International Communications in Heat and Mass Transfer 2018;98:177–82. https://doi.org/10.1016/j.icheatmasstransfer.2018.08.018.
[35] Yaws CL. Transport Properties of Chemicals and Hydrocarbons: Viscosity, Thermal Conductivity, and Diffusivity of C1 to C100 Organics and Ac to Zr Inorganics. Norwich, NY: William Andrew; 2009.
[36] Mannaa O, Mansour MS, Roberts WL, Chung SH. Laminar burning velocities at elevated pressures for gasoline and gasoline surrogates associated with RON. Combustion and Flame 2015;162:2311–21. https://doi.org/10.1016/j.combustflame.2015.01.004.
[37] Ghosh P, Hickey KJ, Jaffe SB. Development of a detailed gasoline composition-based octane model. Industrial & Engineering Chemistry Research 2006;45:337–45. https://doi.org/10.1021/ie050811h.
[38] Al Qubeissi M. Predictions of droplet heating and evaporation: An application to biodiesel, diesel, gasoline and blended fuels. Applied Thermal Engineering 2018;136:260–7. https://doi.org/10.1016/j.applthermaleng.2018.03.010.
[39] Al-Esawi N, Al Qubeissi M, Sazhin SS. The impact of fuel blends and ambient conditions on the heating and evaporation of diesel and biodiesel fuel droplets. 16th International Heat Transfer Conference, Beijing, China: Begellhouse; 2018, p. 6641–8. https://doi.org/10.1615/IHTC16.mpf.020772.
[40] Bader A, Keller P, Hasse C. The influence of non-ideal vapor–liquid equilibrium on the evaporation of ethanol/iso-octane droplets. International Journal of Heat and Mass Transfer 2013;64:547–58. https://doi.org/10.1016/j.ijheatmasstransfer.2013.04.056.
[41] Járvás G, Kontos J, Hancsók J, Dallos A. Modeling ethanol–blended gasoline droplet evaporation using COSMO-RS theory and computation fluid dynamics. International Journal of Heat and Mass Transfer 2015;84:1019–29. https://doi.org/10.1016/j.ijheatmasstransfer.2014.12.046.
[42] Corsetti S, Miles REH, McDonald C, Belotti Y, Reid JP, Kiefer J, et al. Probing the evaporation dynamics of ethanol/gasoline biofuel blends using single droplet manipulation techniques. J Phys Chem A 2015;119:12797–804. https://doi.org/10.1021/acs.jpca.5b10098.
[43] Uslu S, Celik MB. Combustion and emission characteristics of isoamyl alcohol-gasoline blends in spark ignition engine. Fuel 2020;262:116496. https://doi.org/10.1016/j.fuel.2019.116496.
[44] Qian Y, Liu G, Guo J, Zhang Y, Zhu L, Lu X. Engine performance and octane on demand studies of a dual fuel spark ignition engine with ethanol/gasoline surrogates as fuel. Energy Conversion and Management 2019;183:296–306. https://doi.org/10.1016/j.enconman.2019.01.011.
[45] Uslu S, Aydın M. Effect of operating parameters on performance and emissions of a diesel engine fueled with ternary blends of palm oil biodiesel/diethyl ether/diesel by Taguchi method. Fuel 2020;275:117978. https://doi.org/10.1016/j.fuel.2020.117978.
[46] Uslu S. Optimization of diesel engine operating parameters fueled with palm oil-diesel blend: Comparative evaluation between response surface methodology (RSM) and artificial neural network (ANN). Fuel 2020;276:117990. https://doi.org/10.1016/j.fuel.2020.117990.
[47] Department for Transport. Renewable Fuel Statistics 2019. https://www.gov.uk/government/collections/renewable-fuel-statistics (accessed September 20, 2019).
[48] Kuti OA, Sarathy SM, Nishida K. Spray combustion simulation study of waste cooking oil biodiesel and diesel under direct injection diesel engine conditions. Fuel 2020;267:117240. https://doi.org/10.1016/j.fuel.2020.117240.
[49] Al Qubeissi M, Sazhin SS, Crua C, Turner J, Heikal MR. Modelling of biodiesel fuel droplet heating and evaporation: effects of fuel composition. Fuel 2015;154:308–18. https://doi.org/10.1016/j.fuel.2015.03.051.